MODELING ICTAL SENTENCES CHARACTERIZED BY THE OCCURRENCE OF SEIZURES IN A SETTING OF NEUROLOGICAL DISORDER

Orlando Mota Pires[1] - orlando.pires@aln.senaicimatec.edu.br
Adrian Widmer[2] - adrian.widmer@aln.senaicimatec.edu.br
Florêncio Mendes Oliveira Filho[3] - florencio@fieb.org.br
[1]SENAI CIMATEC UNIVERSITY – Salvador – Ba

Abstract.

In this article, we analyze epileptic patients with focal seizures and impaired consciousness using Detrended Fluctuation Analysis (DFA) using Electroencephalogram (EEG) signals. We use an experiment conducted at the Neurology and Neurophysiology Unit of the University of Siena and made available online in the Physionet public database. We report the use of the DFA method to investigate five active channels (F_P1, O_1, C_z, F_P2, O_2) of patients PN00, PN06, and PN07. For analysis purposes, we cut out specific periods as markers for the General, Pre-ictal, Ictal, and Post-ictal phases. To demonstrate the robustness of the technique, we adjust the exponent α_{DFA} for each channel and per phase, revealing the scaling self-affinity at a specific time. Crossovers were identified and tabulated to better configure the α_{DFA} relationship with the signal type. Each phase per patient presented at least two transitions. Responses such as long-range anti-persistent, long-range anti-persistent, long-range persistent, noise ($1/f$), and non-stationary were identified and quantified. Our DFA analysis allowed for better phase segmentation, proved adaptable to the recognition of ictal moments, and revealed the technique's reproducibility for future applications with a larger number of patients.

Keywords: *Epylepsy, Electroencephalogram (EEG), Detrended Fluctuation Analysis (DFA)*

1. INTRODUCTION

Epilepsy is part of a family of neurological disorders that affects millions of people regardless of age, gender, or origin [Scheffer et al. (2017); Steinhoff and Staack (2019)]. It is a chronic neurological condition characterized by the brain's persistent predisposition to generate abnormal and synchronous electrical discharges, resulting in epileptic seizures [Myers et al. (2016)].

These seizures not only represent the clinical hallmark of the disease but are also associated with several negative repercussions, generating cognitive impairment, physical trauma, psychiatric disorders, social difficulties, and, in extreme cases, sudden death [Treiman (2001); Nolan D (2018); Symonds et al. (2017)]. Despite the availability of pharmacological and surgical treatments, approximately 30% of patients remain resistant to conventional therapies [Detti et al. (2020); Amin and Benbadis (2019)]. In this context, seizure anticipation

becomes a promising strategy, as it allows for preventive decisions such as the use of fast-acting medications or the activation of alarm devices [Myers et al. (2016)].

A crucial aspect for advancing prediction strategies is understanding the different phases of the epileptic event: the pre-ictal phase (period before the seizure), the ictal phase (active period of the seizure), and the post-ictal phase (recovery) [Assi et al. (2017); Gadhoumi et al. (2016)]. The pre-ictal phase, in particular, has been the focus of studies due to its potential as a window for intervention. However, accurately identifying this phase is challenging, as its duration and patterns vary between individuals and even between seizures in the same patient. The ictal phase, on the other hand, contains the clinical manifestations of epilepsy and reflects the pathological activation of brain connections. The post-ictal phase, in turn, is marked by changes in the return to basal activity and may provide clues about recovery and regulation mechanisms [Bandarabadi et al. (2015)].

Recent investigations using electroencephalography (EEG), complex networks, and brain synchronization measures reinforce the importance of mapping these transitions for diagnostic and therapeutic purposes, demonstrating that subtle changes in neural connectivity can precede and follow seizure episodes [Treiman (2001); Nolan D (2018); Symonds et al. (2017); Löscher et al. (2020); Campanille et al. (2021)]. These studies suggest that specific patterns of synchronization between brain regions may serve as markers of the different phases of an epileptic seizure [Kramer and Cash (2012); Lemieux et al. (2011); Wendling et al. (2010); Márton et al. (2014)].

Thus, the segmented analysis of the pre-ictal, ictal, and post-ictal phases becomes essential not only to understand the dynamics of epilepsy in greater depth, but also to develop prediction and analysis methods that are more robust, adaptable, and sensitive to critical brain transitions [Myers et al. (2016)]. By accurately identifying the transition moments between these phases, it is possible to significantly improve the accuracy of detection systems and the effectiveness of clinical interventions.

Given the complexity of the context and the need to better understand this neurological disorder via scaling auto-affinity, we sought to add to the literature with a study using the Detrended Fluctuation Analysis (DFA) method, applied to a small sample of patients, as a pilot project, to evaluate the EEG recordings of two male patients (55 and 36 years old) and one female patient (20 years old), both diagnosed with focal seizures with impaired consciousness [Peng et al. (1994); Zebende et al. (2017); Oliveira-Filho et al. (2019); Oliveira Filho (2021); Oliveira Filho et al. (2023); Filho and Zebende (2024); Oliveira Filho et al. (2025); Association. (2001)].

We investigated five channels (F_P1 , O_1, C_z, F_P2, O_2) of EEG distributed throughout the brain in four phases (General, Pre-ictal, ictal, Post-ictal) in a reduced domain of an epileptic episode (first attack) [Detti et al. (2020); PhysioBank (2000); Association. (2001)]. Details of the database, patients chosen, series size, evaluation and transition (crossover) in the exponents α_{DFA} are described and interpreted throughout this study.

2. DATA BANK and METHODS

2.1 DATA BANK

The complete database provides electroencephalographic (EEG) recordings of 14 adult patients, both sexes, obtained at the Neurology and Neurophysiology Unit of the University of

Siena https://www.dsmcn.unisi.it/en. The base consists of 9 men (ages between 25 and 71 years) and 5 women (ages between 20 and 58 years). These patients are monitored via electrodes (10-20 position system) at a sampling rate of 512 Hz. Data were captured using EB Neuro and Natus Quantum LTM amplifiers. All patients were diagnosed with epilepsy according to the criteria of the International League Against Neurological Disorders Characterized by the Occurrence of Seizures (ILAE). https://www.epilepsy.com/.

There are a total of 128 hours of epileptic seizure recordings Detti et al. (2020); PhysioBank (2000). The files are stored in the European Data Format (EDF) and paired with text files detailing the sampling rate, valid channels, and start and end times of the recordings and seizures. Each patient's data is stored in separate folders accompanied by a summary containing metadata Detti et al. (2020); PhysioBank (2000). PENACE projects was responsible for the data collection. https://panacee.diism.unisi.it.

To compose this work, a structured methodology was developed in several stages, including data collection, reading, decompression, and interpretation of the EDF files. The selection and clipping of the series excerpts used were defined using the EDF browser 2.10 software - 64-bit version - https://www.teuniz.net/edfbrowser/. The channels selected for analysis were F_P1 , O_1, C_z, F_P2, O_2. The methodology also meets the rigor with which the experiment was carried out (see folder navigation: https://physionet.org/content/siena-scalp-eeg/1.0.0/). The choice of channels as well as the focus on the first event (study domain) is conclusive for each patient. The figure 1 illustratively demarcates the position of the channels specified above. Figure 2 visually shows the three focal phases (Pre-ictal, ictal, Post-ictal) investigated by the study. The composition of Figure 2 was plotted with the channels of patient PN00.

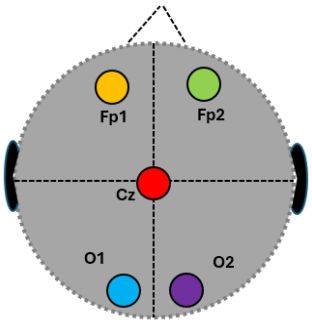

Figure 1: Position of channels FP_1 (yellow), O_1 (blue), C_z (red), FP_2 (green), O_2 (purple) in the brain. System 10 - 20. Detailed illustration can be seen at: https://physionet.org/content/eegmmidb/1.0.0/64_channel_sharbrough.pdf.

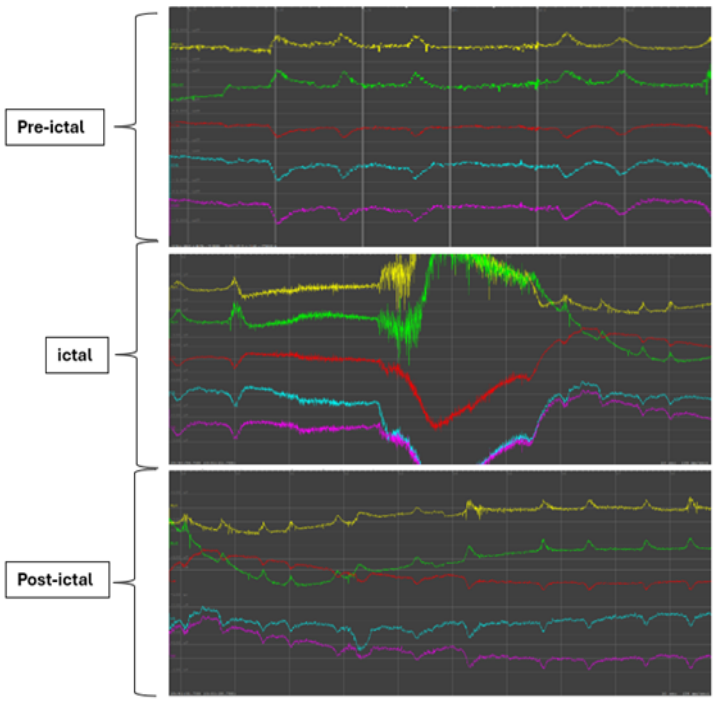

Figure 2: First epileptic episode detected in patient PN00. Phases: Pre-ictal - period immediately preceding the seizure, lasting the same as the seizure itself; Ictal - period corresponding to the seizure event; and Post-ictal: period immediately following the seizure, lasting the same as the ictal period.

Scope delimitation was necessary due to the complexity and analysis of multiple events (patient with more than one attack [PN00 and PN06], both with 5 episodes). Choosing to study the first event allowed for standardization of analyses across patients and ensured greater consistency in results. The patients were:

- Patient PN00, male, 55 years old, 198 minutes, focal onset with impaired consciousness (IAS), temporal location, right side and presenting 5 epileptic episodes throughout the entire observation period `https://physionet.org/content/siena-scalp-eeg/1.0.0/PN00/Seizures-list-PN00.txt`. Registration start time: 19:39:33. Registration end time: 20:22:58. Seizure start time: 19:58:36. Seizure end time: 19:59:46.
- Patient PN06, male, 27 years old, 722 minutes, focal onset with impaired consciousness (IAS), temporal location, left side and presenting 5 epileptic episodes throughout the entire observation period `https://physionet.org/content/siena-scalp-eeg/1.0.0/PN06/Seizures-list-PN06.txt`. Registration start time: 04.21.22. Registration end time: 07.01.37. Seizure start time: 05.54.25. Seizure end time: 05.55.29.
- Patient PN07, male, 20 years old, 523 minutes, focal onset with impaired consciousness (IAS), temporal location, left side and presenting 1 epileptic episode throughout the entire observed period `https://physionet.org/content/siena-scalp-eeg/1.0.0/PN07/Seizures-list-PN07.txt`. Registration start time: 23.18.10. Registration end time: 08.01.58. Seizure start time: 05.25.49. Seizure end time: 05.26.51.

2.2 Detrended Fluctuation Analysis (DFA)

To understand the method proposed by Peng1994, in summary, consider a time series $\{u_i\}$ (electric potential), with $i = 1, \cdots, N_{max}$ (time series length N_{max}). Therefore, the next step to understanding the DFA method is to determine the deviations from the mean $\langle u \rangle$, thus obtaining the new integrated time series, by:

$$y(k) = \sum_{i=1}^{k} [u_i - \langle u \rangle] \tag{1}$$

with $k = 1, \ldots, N_{max}$.

The integrated time series, $y(k)$, is divided into bins of equal size n. For each bin of size n, a polynomial of degree 1 is obtained by the least squares method. This fit gives the local trend, $y_n k$, in each bin. Now, the integrated time series, $y(k)$, is subtracted from $y_n k$ in each bin of size n (time scale). Then, the root-mean-square fluctuation function, $F_{DFA}(n)$, is calculated by:

$$F_{DFA}(n) = \sqrt{\frac{1}{N_{max}} \sum_{k=1}^{N_{max}} [y(k) - y_n(k)]^2} \tag{2}$$

The above calculation is repeated for a wide range of timescales, i.e., $4 \leq n \leq \frac{N_{max}}{4}$. If F_{DFA} follows a power law as a function of time scale n, then:

$$F_{DFA}(n) \sim n^{\alpha_{DFA}} \tag{3}$$

With α_{DFA} defined as the autocorrelation exponent, or the long-range correlation indicator, see Table 1 and [Walleczek (2006); Zebende et al. (2016)] for more details.

Table 1: DFA exponent and its type of signal.

DFA exponent	**type of signal**
$\alpha_{DFA} < 0.5$	long-range anti-persistent
$\alpha_{DFA} \simeq 0.5$	uncorrelated (white noise)
$\alpha_{DFA} > 0.5$	long-range persistent
$\alpha_{DFA} \simeq 1$	$1/f$ noise
$\alpha_{DFA} > 1$	non-stationary
$\alpha_{DFA} \simeq 3/2$	brownian noise

We can cite more articles that applied the DFA method to analyze EEG signals, including [Zebende et al. (2017); Oliveira-Filho et al. (2019); Mesquita et al. (2020); Filho and de Santana (2022); Oliveira Filho (2021); Oliveira Filho et al. (2023); Filho and Zebende (2024); Oliveira Filho et al. (2025); Márton et al. (2014)].

3. RESULTS

For analysis purposes, we investigated the effect of autocorrelation via the DFA method on neurological disorders caused by electrical impulse disorders (epilepsy) in three patients (PN00, PN06, and PN07) out of a total of 14. The database is in the public domain and available to researchers in the Physionet repository `https://physionet.org/content/siena-scalp-eeg/1.0.0/`. We chose 5 EEG channels (F_P1, O_1, C_z, F_P2, O_2) distributed among the regions: frontal lobe (F_P1 and F_P2), central (C_z), and occipital (O_1, O_2). The choice of channels was defined visually using teuniz.net software. The database provides a total of 29 EEG channels.

For each patient, the first epileptic episode was observed with a specific Δt(seconds) per patient (temporal domain). Figure 2 allowed visualizing the variability of the epileptic seizure as a function of the discharge time. Specific periods were selected to characterize the moments before the discharge, during the discharge, and after the discharge. Figure 3 was generated to highlight these moments. Each slice had 153,601 points, equivalent to a time of $\sim$ 30 seconds (153,601 * 0.0019534). We observed that the period defined as the discharge time was longer than the time observed visually via the software `https://www.teuniz.net/edfbrowser/`. We chose the observed time ($\sim$ 30 seconds). The table 2 shows the original times compared to the observed seizure time.

Using DFA, we calculated the autocorrelation for the five channels (F_P1, O_1, C_z, F_P2, O_2) in the pre-ictal, ictal, and post-ictal periods. For clarity, we added the Total time (see figures 4, 5, and 6). The Total time was inserted as a comparative phase in relation to the ictal phases. In total, 64 curves were fitted using exponent α_{DFA}. Based on the expected fit of the method, crossover points were visualized. Tables 3, 4, and 5 show the adjustments made. The relationship between alphas and signal type can be interpreted from table 1.

In the individual analysis of patients PN00, PN06, and PN07, we observed that:

PN00: Table 3. Two moments were adjusted for all phases (Total, Pre-ictal, ictal and Post-ictal). In the Total phase, non-stationary behavior was observed throughout the interval 4 - 1200, with the exception of channel F_P1 which revealed a persistent regime. In the Pre-ictal phase, interval between 4 - 40, persistent behavior was observed for channels F_P1, O_1, C_z and O_2, while F_P2 presented non-stationary behavior. For the Pre-ictal phase interval $>$ 40, non-stationary behavior was observed for C_z, F_P2 and O_2, accompanied by long-range persistent for F_P1 and noise for O_1. In the ictal phase, in the interval 4-200, the regime was non-stationary for all channels, followed by long-range persistent for all channels in the interval $>$ 200. Finally, the post-ictal phase presented long-range anti-persistent behavior in the interval 4-40, followed by non-stationary behavior for the interval $>$ 40.

PN01: Table 4. The adjustment was made in three moments for the Total phase, two moments in the Pre-ictal phase, two moments for the ictal phase, and three moments for the Post-ictal phase. In the Total phase, in the interval 4-30, F_P1, C_z, and F_P2 presented long-range persistent behavior, while O_1 and O_2 were non-stationary. In the range between 30 - 1100, F_P1 and F_P2 behaved non-stationary, C_z with long-range persistent, O_1 long-range anti-persistent and O_2 uncorrelated (white noise). Still in Total, range $>$ 1100, F_P1, C_z, F_P2 presented long-range persistent, O_1 long-range anti-persistent and O_2 uncorrelated (white noise). In the pre-ictal period, there is a clear transition from non-stationary behavior (4 - 600) to long-range anti-persistent behavior (interval $>$ 600) in the channels (F_P1, O_1,

O_2) and uncorrelated (white noise) (C_z, F_P2). In the ictal phase, interval 4 - 30, long-range persistent behavior occurs in the channels F_P1, O_1 and F_P2, while C_z and O_2 are non-stationary. In the interval $>$ 30, long-range persistent behavior occurs for F_P1 and O_2, accompanying O_1, C_z and F_P2 with non-stationary behavior. Finally, in the post-ictal phase, interval 4 - 30, long-range persistent behavior is observed for F_P1, O_2, F_P2, and C_z, accompanied by O_2 with uncorrelated (white noise). In the interval 30 - 2000, non-stationary behavior is observed for channels F_P1, O_1, F_P2, and C_z, except for O_2 with long-range persistent behavior. In the interval $>$ 2000, long-range anti-persistent behavior is observed for F_P1, long-range persistent behavior for F_P1 and O_1, and non-stationary behavior for C_z and O_2.

PN07: Table 5. In this patient, the adjustment occurred in two moments for the Total phase, four moments in the Pre-ictal phase, two moments for ictal and three moments for Post-ictal. In the Total phase, in both intervals the long-range persistent behavior was presented in all channels, with the exception of channel O_2 which revealed non-stationary behavior in values $>$ 13. The Pre-ictal phase was marked by variations from long-range persistent ($\alpha_{DFA} > 0.5$) to long-range anti-persistent ($\alpha_{DFA} < 0.5$), followed by non-stationary $\alpha_{DFA} > 1$ and finally long-range persistent ($\alpha_{DFA} > 0.5$) in channel F_P1. The others also followed the same reasons, however, presenting a phase with a different signal type. In the ictal phase, in the interval 4 - 154, we observed non-stationary behavior in the channels F_P1, O_2, F_P2 and C_z and long-range anti-persistent in O_1. In the interval $>$ 154, long-range persistent for all channels. Finally, in the Post-ictal phase, in the interval 4 - 11, long-range anti-persistent behavior in O_1, F_P2, O_2 and long-range persistent in F_P1 and C_z. In the range 11 - 119, long-range anti-persistent behavior in C_z, F_P1, O_2 and long-range persistent behavior in F_P2 and O_1. In the last Post-ictal phase, interval $>$ 119, long-range persistent for C_z, F_P1, O_1, O_2 and long-range anti-persistent for F_P2.

Table 2: Information on epileptic seizure records - first discharge per patient. Data available in (folders): `https://physionet.org/content/siena-scalp-eeg/1.0.0/`.

Seizure	Registration start	Registration end	Seizure start	Seizure end
PN00	19:39:33	20:22:58	19:58:36	19:59:46
PN06	04:21:22	07:01:37	05:54:25	05:55:29
PN07	23:18:10	08:01:58	05:25:49	05:26:51

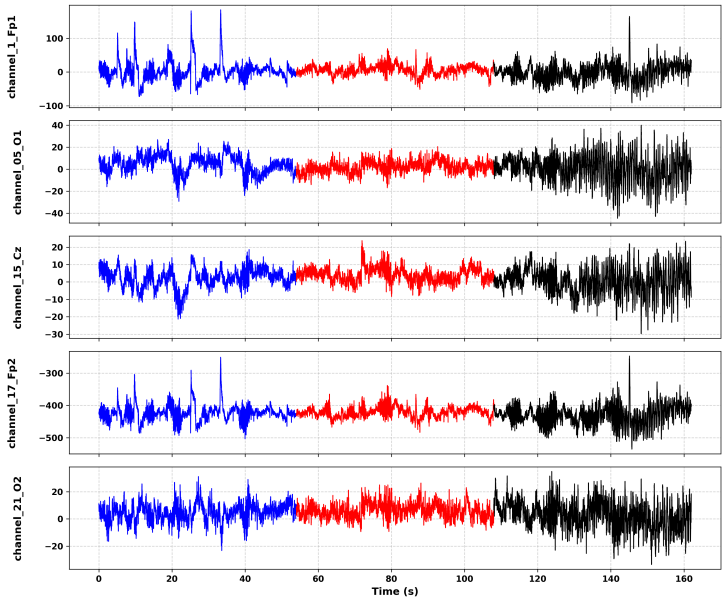

Figure 3: Image of pre-ictal (blue), ictal (red) and post-ictal (black) states. Record PN00, patient with focal onset and impaired consciousness. 55 years old, Male, temporal region, Right side. Approximately 198 seconds of observation. Path: `https://physionet.org/content/siena-scalp-eeg/1.0.0/subject_info.csv`. Excerpts cropped for easier viewing - Software: EDFbrowser 2.10 - 64-bit version - `https://www.teuniz.net/edfbrowser/`.

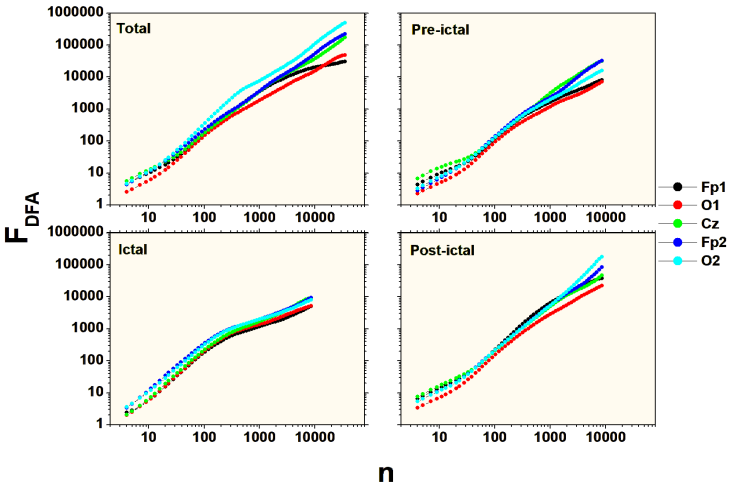

Figure 4

Table 3: **PN00**: (Adjustment in the trend of the channels F_P1, O_1, C_z, F_P2 and O_2 via DFA method. The subtlety of the behavioral adjustments are made depending on the transition point between scale periods (Crossover). The sign of (✓) in the context of the table means that the adjustment made previously will be maintained for the subsequent interval.)

Channel	Total 4–1200	Total > 1200	Pre-ictal 4–40	Pre-ictal > 40	Ictal 4–200	Ictal > 200	Post-ictal 4–40	Post-ictal > 40
Fp1	1.28 ± 0.01	0.54 ± 0.02	0.79 ± 0.01	0.99 ± 0.02	1.41 ± 0.02	0.61 ± 0.01	0.88 ± 0.01	1.24 ± 0.02
O1	1.06 ± 0.01	✓	0.96 ± 0.03	1.00 ± 0.02	1.47 ± 0.01	0.60 ± 0.00	1.00 ± 0.03	1.17 ± 0.01
Cz	1.18 ± 0.00	✓	0.70 ± 0.01	1.29 ± 0.01	1.46 ± 0.01	0.75 ± 0.01	0.84 ± 0.01	1.25 ± 0.01
Fp2	1.21 ± 0.00	✓	1.06 ± 0.02	1.24 ± 0.01	1.42 ± 0.01	0.63 ± 0.01	0.97 ± 0.03	1.33 ± 0.01
O2	1.29 ± 0.01	✓	0.97 ± 0.02	1.11 ± 0.01	1.40 ± 0.01	0.60 ± 0.00	0.96 ± 0.03	1.48 ± 0.01

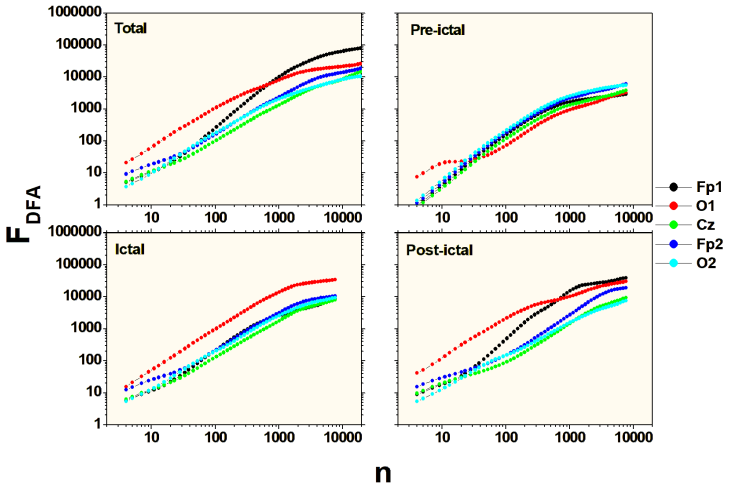

Figure 5

Table 4: **PN06**: (Adjustment in the trend of the channels FP_P1, O_1, C_z, F_P2 and O_2 via DFA method. The subtlety of the behavioral adjustments are made depending on the transition point between scale periods (Crossover). The sign of (✓) in the context of the table means that the adjustment made previously will be maintained for the subsequent interval.)

Canal	Total 4 – 30	Total 30 – 1100	Total > 1100	Pre-ictal 4 – 600	Pre-ictal > 600	Ictal 4 – 30	Ictal > 30	Post-ictal 4 – 30	Post-ictal 30 – 2000	Post-ictal > 2000
Fp1	0.92 ± 0.03	1.52 ± 0.01	0.56 ± 0.02	1.45 ± 0.02	0.31 ± 0.01	0.86 ± 0.03	0.95 ± 0.03	0.86 ± 0.03	1.51 ± 0.02	0.34 ± 0.01
O1	1.07 ± 0.02	0.33 ± 0.01	✓	1.04 ± 0.05	0.31 ± 0.04	0.92 ± 0.02	1.13 ± 0.00	0.50 ± 0.01	1.20 ± 0.01	0.55 ± 0.00
Cz	0.96 ± 0.01	✓	✓	1.41 ± 0.01	0.52 ± 0.00	1.04 ± 0.01	✓	0.67 ± 0.01	1.09 ± 0.01	✓
Fp2	0.71 ± 0.01	1.17 ± 0.00	0.63 ± 0.02	1.44 ± 0.01	0.52 ± 0.01	0.70 ± 0.01	1.02 ± 0.02	0.63 ± 0.01	1.20 ± 0.01	0.55 ± 0.05
O2	1.17 ± 0.01	0.50 ± 0.01	✓	1.43 ± 0.02	0.44 ± 0.01	1.44 ± 0.00	0.60 ± 0.02	0.98 ± 0.01	✓	✓

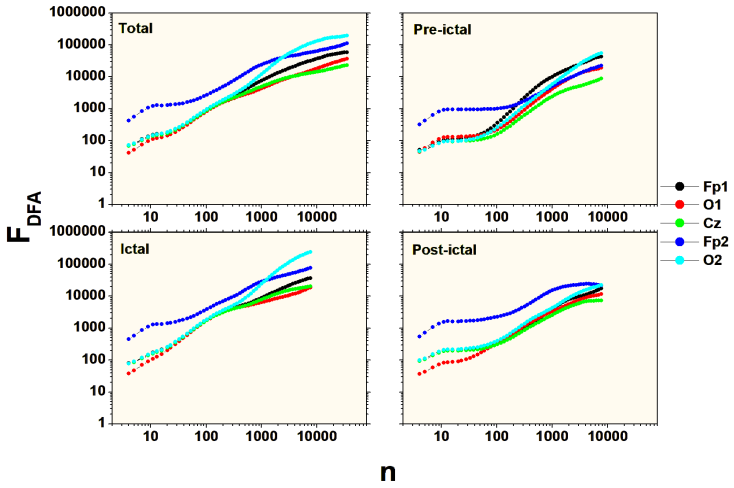

Figure 6

Table 5: **PN07**: (Adjustment in the trend of the channels FP_1, O_1, C_z, FP_2 and O_2 via DFA method. The subtlety of the behavioral adjustments are made depending on the transition point between scale periods (Crossover)).

Canal	Total 4–13	Total > 13	Pre-ictal 4–11	Pre-ictal 11–69	Pre-ictal 69–723	Pre-ictal > 723	Ictal 4–154	Ictal > 154	Post-ictal 4–11	Post-ictal 11–119	Post-ictal > 119
Fp1	0.71 ± 0.03	0.80 ± 0.01	0.72 ± 0.02	0.33 ± 0.04	1.55 ± 0.01	0.76 ± 0.01	1.35 ± 0.01	0.67 ± 0.01	0.77 ± 0.03	0.23 ± 0.03	0.94 ± 0.02
O1	0.93 ± 0.06	0.72 ± 0.01	1.05 ± 0.06	0.12 ± 0.02	1.26 ± 0.01	0.65 ± 0.03	0.18 ± 0.02	0.86 ± 0.01	0.48 ± 0.01	0.94 ± 0.02	0.86 ± 0.01
Cz	0.69 ± 0.03	0.65 ± 0.01	0.71 ± 0.03	0.21 ± 0.03	1.22 ± 0.00	0.58 ± 0.01	1.45 ± 0.01	0.68 ± 0.01	0.74 ± 0.03	0.21 ± 0.02	0.80 ± 0.02
Fp2	0.96 ± 0.08	0.64 ± 0.01	1.07 ± 0.06	0.10 ± 0.02	0.82 ± 0.01	1.00 ± 0.01	1.39 ± 0.06	0.77 ± 0.01	0.16 ± 0.01	0.89 ± 0.01	0.07 ± 0.02
O2	0.70 ± 0.03	1.12 ± 0.01	0.44 ± 0.02	0.70 ± 0.03	0.39 ± 0.05	1.30 ± 0.01	1.40 ± 0.01	0.70 ± 0.01	0.01 ± 0.03	0.30 ± 0.03	0.96 ± 0.01

4. CONCLUSIONS

In this research, we evaluated EEG data from a public database provided by the Neurology and Neurophysiology Unit of the University of Siena. Our reduced-domain analysis included the participation of three epileptic patients (PN00, PN06, and PN07) with focal seizures and impaired consciousness. Five channels (F_P1, O_1, C_z, F_P2, O_2) distributed among the frontal lobe (F_P1 and F_P2), central (C_z), and occipital (O_1, O_2) regions were investigated. Using the DFA method, we investigated the autocorrelation of the time series to understand the phase changes (General, Pre-ictal, Ictal, and Post-ictal), as well as the transitions (Crossover). For analysis purposes, the study considered the first discharge of each patient.

Using the DFA method, we observed that the tracing and behavior depend on the patient, discharge time, and their phase transitions. For each patient, we adjusted the exponent α_{DFA} to the signal type and observed how each adjustment behaved. The analysis presented here is short in number of subjects but rich in detail. As a perspective, we believe that the study can be replicated for the 14 patients in the database made available using this methodology, as well as for other databases and neurological disorders that use EEG as a reference for physiological measurement.

Acknowledgements

Florencio Mendes Oliveira Filho thanks Senai Cimatec University and the National Council for Scientific and Technological Development (CNPq) scholarship 150655/2022-3.

REFERENCES

Amin, U. and Benbadis, S. R. (2019). The role of eeg in the erroneous diagnosis of epilepsy. *Journal of clinical neurophysiology*, 36(4):294–297.

Assi, E. B., Nguyen, D. K., Rihana, S., and Sawan, M. (2017). Towards accurate prediction of epileptic seizures: A review. *Biomedical Signal Processing and Control*, 34:144–157.

Association., W. M. (2001). World medical association declaration of helsinki. ethical principles for medical research involving human subjects. *Bulletin of the World Health Organization*, 79(4):373 – 374.

Bandarabadi, M., Rasekhi, J., Teixeira, C. A., Karami, M. R., and Dourado, A. (2015). On the proper selection of preictal period for seizure prediction. *Epilepsy & Behavior*, 46:158–166.

Campanille, V., Sierra, N., Calle, A., Bernater, R., Thomson, A., et al. (2021). La epilepsia mioclónica juvenil y las disfunciones neurocognitivas y ejecutivas asociadas. *MEDICINA (Buenos Aires)*, 81(6):965–971.

Detti, P., Vatti, G., and Zabalo Manrique de Lara, G. (2020). Eeg synchronization analysis for seizure prediction: A study on data of noninvasive recordings. *Processes*, 8(7).

Filho, F. M. O. and de Santana, J. P. C. (2022). Difference in the Range of Floating in Individuals Diagnosed with Amyotrophic Lateral Sclerosis: A preliminary study with the rms float function. *International Journal of Research in Engineering and Science*.

Filho, F. M. O. and Zebende, G. F. (2024). Temporal coherence in the synchronization of brain electrical activity patterns: An application with the rms fluctuation function. *Journal ISSN*, 2766:2276.

Gadhoumi, K., Lina, J.-M., Mormann, F., and Gotman, J. (2016). Seizure prediction for therapeutic devices: A review. *Journal of neuroscience methods*, 260:270–282.

Kramer, M. A. and Cash, S. S. (2012). Epilepsy as a disorder of cortical network organization. *The Neuroscientist*, 18(4):360–372.

Lemieux, L., Daunizeau, J., and Walker, M. C. (2011). Concepts of connectivity and human epileptic activity. *Frontiers in systems neuroscience*, 5:12.

Löscher, W., Potschka, H., Sisodiya, S. M., and Vezzani, A. (2020). Drug resistance in epilepsy: clinical impact, potential mechanisms, and new innovative treatment options. *Pharmacological reviews*, 72(3):606–638.

Márton, L., Brassai, S. T., Bakó, L., and Losonczi, L. (2014). Detrended fluctuation analysis of eeg signals. *Procedia Technology*, 12:125–132.

Mesquita, V. B., Oliveira-Filho, F. M., and Rodrigues, P. C. (2020). Detection of crossover points in detrended fluctuation analysis: An application to EEG signals of patients with epilepsy. *Bioinformatics*.

Myers, M. H., Padmanabha, A., Hossain, G., de Jongh Curry, A. L., and Blaha, C. D. (2016). Seizure prediction and detection via phase and amplitude lock values. *Frontiers in human neuroscience*, 10:80.

Nolan D, F. J. (2018). Genetics of epilepsy. *Handb Clin Neurol*, (148):467–491.

Oliveira Filho, e. a. (2021). Self-regulation in electroencephalographic signals during an arithmetic performance test: an approach with an rms fluctuation function. *15921091210*, 9(15921091210).

Oliveira Filho, F., Ribeiro, F., Cruz, J. L., de Castro, A. N., and Zebende, G. (2023). Statistical study of the eeg in motor tasks (real and imaginary). *Physica A: Statistical Mechanics and its Applications*, 622:128802.

Oliveira Filho, F. M., dos Santos Silva, E. F., de Freitas Santos, S. E., Bandeira Santos, A. Á., and Zebende, G. F. (2025). Study of autocorrelations and uncertainties applied to patients with parkinson's disease. *Scientific Reports*, 15(1):10068.

Oliveira-Filho, F. M., Leyva-Cruz, J. A., and Zebende, G. F. (2019). Analysis of the EEG bio-signals during the reading task by DFA method. *Physica A*, 525:664 – 671.

Peng, C. K., Buldyrev, S. V., Havlin, S., Simons, M., Stanley, H. E., and Goldberger, A. L. (1994). Mosaic organization of DNA nucleotides. *Phys. Rev. E*, 49:1685–1689.

PhysioBank, P. (2000). Physionet: components of a new research resource for complex physiologic signals. *Circulation*, 101(23):e215–e220.

Scheffer, I. E., Berkovic, S., Capovilla, G., Connolly, M. B., French, J., Guilhoto, L., Hirsch, E., Jain, S., Mathern, G. W., Moshé, S. L., et al. (2017). Ilae classification of the epilepsies: Position paper of the ilae commission for classification and terminology. *Epilepsia*, 58(4):512–521.

Steinhoff, B. J. and Staack, A. M. (2019). Is there a place for surgical treatment of nonpharmacoresistant epilepsy? *Epilepsy & Behavior*, 91:4–8.

Symonds, J. D., Zuberi, S. M., and Johnson, M. R. (2017). Advances in epilepsy gene discovery and implications for epilepsy diagnosis and treatment. *Current opinion in neurology*, 30(2):193–199.

Treiman, D. M. (2001). Gabaergic mechanisms in epilepsy. *Epilepsia*, 42:8–12.

Walleczek, J. (2006). *Self-organized biological dynamics and nonlinear control: toward understanding complexity, chaos and emergent function in living systems*. Cambridge University Press.

Wendling, F., Chauvel, P., Biraben, A., and Bartolomei, F. (2010). From intracerebral eeg signals to brain connectivity: identification of epileptogenic networks in partial epilepsy. *Frontiers in systems neuroscience*, 4:154.

Zebende, G. F., Fernandez, B. F., and Pereira, M. G. (2016). Analysis of the variability in the sdB star KIC 10670103: DFA approach. *Monthly Notices of the Royal Astronomical Society*, 464(3):2638–2642.

Zebende, G. F., Oliveira-Filho, F. M., and Leyva-Cruz, J. A. (2017). Auto-correlation in the motor/imaginary human EEG signals: A vision about the FDFA fluctuations. *PLOS ONE*, 12(9).